PROGRESS IN COLOR, COLORANTS AND COATINGS

available online @ www.pccc.icrc.ac.ir

Ministry of Science, Research and Technology
Institute for Color Science & Technology

Progress in Color Colorants Coating 16 (2023), 59-70

Antibacterial Corrosion Inhibitor for the Protection of Mild Steel in 1 M HCl Solution

S. S. Hussein[1], I. D. D. Al-Hasani[2], A. M. Abed[3], M. M Hanoon[4], L. M. Shaker[5], A. A. Alamiery[5, 6*], A. A. H. Kadhum[7], W. N. Roslam Wan Isahak[5]

[1.] Department of Chemical Engineering, University of Technology, P. O. Box: 10001, Baghdad, Iraq
[2.] Technical Hospital Al-Muthana, Ministry of Health, P. O. Box: 66002, Al-Muthana, Iraq
[3.] Air Conditioning and Refrigeration Technology Department, Al-Mustaqbal University College, P. O. Box: 51001, Babylon, Iraq
[4.] Department of Production Engineering and Metallurgy, University of Technology, Baghdad, P. O. Box: 10001, Iraq
[5.] Department of Chemical and Process Engineering, Faculty of Engineering and Built Environment, Universiti Kebangsaan Malaysia (UKM), P.O. Box: 43000, Bangi 43600, Selangor, Malaysia
[6.] Energy and Renewable Energies Technology Center, University of Technology, P. O. Box: 10001, Baghdad, Iraq
[7.] Department of Medicine, University of Al-Ameed, P. O. Box: 56001, Karbala, Iraq

ARTICLE INFO

Article history:
Received: 07 Jan 2022
Final Revised: 14 Mar 2022
Accepted: 18 Mar 2022
Available online: 10 Oct 2022

Keywords:
Corrosion inhibitor
DFT
Gravimetric
P-CBHM
Mild steel

ABSTRACT

Mild steel is widely utilised as a construction material because of its mechanical qualities and low cost but its weak acid corrosion resistance limits its application. The ability of para-chlorobenzoyl-hydrazinylmethane (P-CBHM) as a corrosion inhibitor and antibacterial agent was investigated by gravimetric measurements, density functional theory (DFT) and antibacterial studies. The weight loss results showed that the inhibition efficiency of P-CBHM to prevent the corrosion of mild steel in 1.0 M HCl increased with concentration from 100 to 500 ppm, with a maximum inhibition efficiency of 96.5 % at 500 ppm. The inhibitory action of the inhibitor was explained in terms of adsorption on the mild steel surface which follows a Langmuir isotherm via physisorption and chemisorption mechanisms. P-CBHM has significant corrosive protection efficacy and antimicrobial activity similar to the common antibacterial agent, chloramphenicol. The novelty of this work was the investigation of the protective response of P-CBHM which was analysed analytically on the corrosion of mild steel in 1.0 M hydrochloric acid using gravimetric and thermometric techniques and its antibacterial effects. Prog. Color Colorants Coat. 16 (2023), 59-70© Institute for Color Science and Technology.

1. Introduction

The increasing incidence of hard-to-diagnose and multidrug-resistant diseases is a major public health concern, therefore there is an urgent need to develop new, safe and effective antimicrobial drugs. Synthesis of new chemical compounds, which may lead to broad modes of action and be less toxic to humans, is among the various approaches to identify new targeted therapies. Hydrazine molecules are major antibacterial agents and the $CO\text{-}CH_2\text{-}NH\text{-}NH_2$ part is important because of its potential biological activity (Figure 1). Due to their high corrosion resistance, poisonous organic compounds containing N, O, and S are widely utilised as corrosion inhibitors, providing protection by preventing

*Corresponding author: * dr.ahmed1975@ukm.edu.my
dr.ahmed1975@gmail.com
Doi: 10.30509/pccc.2022.166935.1149

contact between the metallic surface and the corrosive environment through an absorption mechanism. In contrast, synthetic organic molecules are both environmentally unfriendly and expensive, limiting their utility in practical applications. Due to their cost-effectiveness and environmental friendliness, green-inhibitors have received increasing attention in recent decades to overcome the constraints of standard synthetic inhibitors. To gain a better understanding of how organic compounds suppress corrosion, it is important to investigate the adsorption mechanism of these molecules on the metal surface. The efficacy of most organic corrosion inhibitors is typically related to their adsorption capabilities at the metal/solution interface, thus may be investigated using adsorption isotherms which can reveal more about the adsorption mechanism as well as the types of interactions that occur between the inhibitors and the steel surface. Indeed, corrosion inhibitors can adsorb at the interface via two types of interactions: physical adsorption (weak interactions) resulting from electrostatic interactions between charged molecules and the metal surface, and chemical adsorption resulting from electron sharing between inhibitors and d-orbitals of the iron surface.

The commonly used mild steel is particularly susceptible to corrosion in acidic solutions, therefore, using efficient strategies to impede the acidic mild steel corrosion is important [1-4]. Typically, natural inhibitors containing various functional groups like heteroatoms (nitrogen, oxygen, sulphur and phosphorous), π-bond, in addition to polar sites are applied to shield the mild steel surface from corrosion through developing an adsorbed layer on the metal surface as these functional groups can facilitate in the physisorption and/or chemisorption of inhibitors on the metal surface [5-9]. Unfortunately, some conventional organic inhibitors are no longer appropriate as they are harmful to the environment and living organisms [10-14], therefore scientists have been working to develop eco-friendly corrosion inhibitors [15-17] to block or retard mild steel substrate acidic corrosion [18], for example, functionalized polymer nanocomposites as anti-corrosion coatings [19]. However, due to their laborious and costly synthesis methods or short shelf life, the application of various organic inhibitors is still restricted. Consequently, the main objective of this study was to investigate the corrosion process of mild steel in 1 M hydrochloric acid solution in the absence and presence of different concentrations of a novel corrosion inhibitor, para-chlorobenzoylhydrazinylmethane (*P*-CBHM) (Figure 1). The antibacterial effects of *P*-CBHM were also investigated.

2. Experimental

2.1. Materials

Mild steel samples were purchased from the Company of Metal Samples and their chemical composition is shown in Table 1. The samples were cleaned according to the standard method G1-03/ASTM [20]. The corrosive solution was prepared by diluting 37 % HCl (Merck-Malaysia) with distilled water.

2.2. Gravimetric techniques

Hydrochloric acid (1 M) was prepared for the corrosion measurements. The mild steel stips were cut into samples measuring 4.5 × 2 × 0.5 mm, rinsed with bidistilled water and acetone, then dried in an oven. The samples were soaked in 1 M HCl media without and with the addition of *P*-CBHM (100, 200, 300, 400, and 500 ppm) at room temperature for 1, 5, 10, and 24 h. The mild steel sample mass loss was based on the total area [21-26], with the corrosion rate (C_R), protection efficiency (IE %) and surface coverage degree (θ) calculated as follows (Eqs. 1-3) [21-26]:

$$C_R = \frac{W_L}{at} \quad (1)$$

$$IE\% = \left[\left(1 - \frac{w_{inh}}{w_{blank}}\right) \times 100\right] \quad (2)$$

$$\theta = \left[1 - \frac{w_{inh}}{w_{blank}}\right] \quad (3)$$

To ensure the accuracy of the weight loss results, the mild steel samples were weighed three times to determine the average. The corrosion rates of the samples at different temperatures were tested (303, 313, 323, 333 K) at 5 h as the optimum immersion time, and the temperature of the hydrochloric acid solution was regulated by placing the corrosion container in the furnace at a constant temperature [27-29].

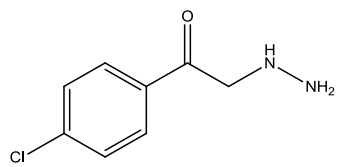

Figure 1: The P-CBHM molecular structure.

Table 1: Chemical composition of the mild steel sample (wt.%).

Carbon	Manganese	Silicon	Aluminium	Sulphur	Phosphorus	Iron
0.210	0.050	0.380	0.010	0.050	0.090	balance

2.3. Theoretical study

The density functional theory (DFT) with the B3LYP hybrid with the basis set 6-311^{++}G was used to evaluate the theoretical chemical factors [30-33]. The computation characteristics of *P*-CBHM molecules cover the frontier molecular orbitals (HOMO, and LUMO), energy gap ($\Delta E = E_{HOMO} - E_{LUMO}$), ionization energy (I), electronic affinity (A), electronegativity (χ), hardness (η), softness (S), and the fraction of electron transfer (ΔN) which were determined according to Eqs. 4-9 [34]:

$$I = -HOMO \quad (4)$$

$$A = -LUMO \quad (5)$$

$$\chi = \frac{E_{HOMO}+E_{LUMO}}{2} \quad (6)$$

$$\eta = -\frac{E_{HOMO}-E_{LUMO}}{2} \quad (7)$$

$$S = \frac{1}{\eta} \quad (8)$$

$$\Delta N = \frac{4.82-\chi_{P-CBHM}}{2(\eta_{P-CBHM})} \quad (9)$$

HOMO and LUMO are the highest occupied molecular orbital and lowest unoccupied molecular orbital, respectively.

2.4. Antibacterial study

The antimicrobial activity of *P*-CBHM compared to the standard medicinal medication chloramphenicol (positive control) was assessed via a disc diffusion method using the gram-negative *P. vulgaris*, *E. coli*, *P. aeruginosa* and *K. pneumonia* and gram-positive *S. aureus.* Various concentrations of *P*-CBHM were prepared using dimethylformamide (100, 200, 300, 400, 500 and 1000 ppm) and the pathogens were cultured in nutritional media. The *P*-CBHM was applied to 6-mm filter paper (Whatman No. 4) discs, then mounted singly and cultured in Petri dishes for 24 hours at 37 °C. The antibacterial effectiveness was calculated according to [35].

3. Results and Discussion

3.1. Effect of concentration and immersion period

Figure 2 presents the corrosion rates (C_R) and the inhibitory efficacies (*IE* %) of mild steel exposed to corrosive medium without and with the addition of *P*-CBHM (100, 200, 300, 400, 500 and 1000 ppm) for various immersion periods at 303 K. temperature. The (C_R) reduces as the *P*-CBHM concentration increases, indicating that a huge number of *P*-CBHM molecules have been adsorbed by the sample surface hence decreasing the contact between the corrosive HCl and mild steel surface. Moreover, the inhibitive efficacy increased with the increasing *P*-CBHM concentration due to the coordination bond formation between the unshared ion pairs of the oxygen and nitrogen atoms and the d-orbitals of Fe atoms on the sample surface, thereby improving the protection performance of the *P*-CBHM.

Moreover, the corrosion inhibition behaviour of *P*-CBHM (IE %) increased dramatically as the exposure period increased (Figure 2), showing that adsorbed *P*-CBHM is continuously covering the mild steel surface. In this instance, mild steel corrosion occurs solely on the exposed sample surface or the pores of the adsorbed coating [36, 37]. The corrosion rate reduced in the first 10 h of exposure and the inhibitive efficacy increased as the immersion time increased, indicating continued *P*-CBHM adsorption on the sample surface. C_R and IE % achieved a steady state as the immersion time increased. The corrosion rate increased slightly after 24 h of immersion, while the inhibitive efficacy reduced due to the dissociation of the protective layer on the mild steel surface. The greatest inhibition efficiency of 96.5 % was achieved in the presence of 500 ppm *P*-CBHM, due to the *P*-CBHM molecules being adsorbed at the corrosion sites of the mild steel surface. The mild steel becomes inhibited and the adsorbed coating forms a protective film between the mild steel and the corrosive solution. A further increase in concentration does not improve inhibition beyond the optimum value. Indeed, the corrosion rate of mild steel decreases from 24.5 to 5.5 mmy^{-1} on the addition of 100 ppm to 500 ppm of *P*-

CBHM, possibly due to the increased absorption and increased coverage of *P*-CBHM on the mild steel surface with an increasing concentration of *P*-CBHM. The inhibition efficiency with various immersion times from 1 to 48 h at 500 ppm *P*-CBHM is shown in Figure 2. The IE % increased from 84 to 96 % when the immersion time increased from 1 to 5 h with no further change observed when the immersion time increased from 5 to 10 h.

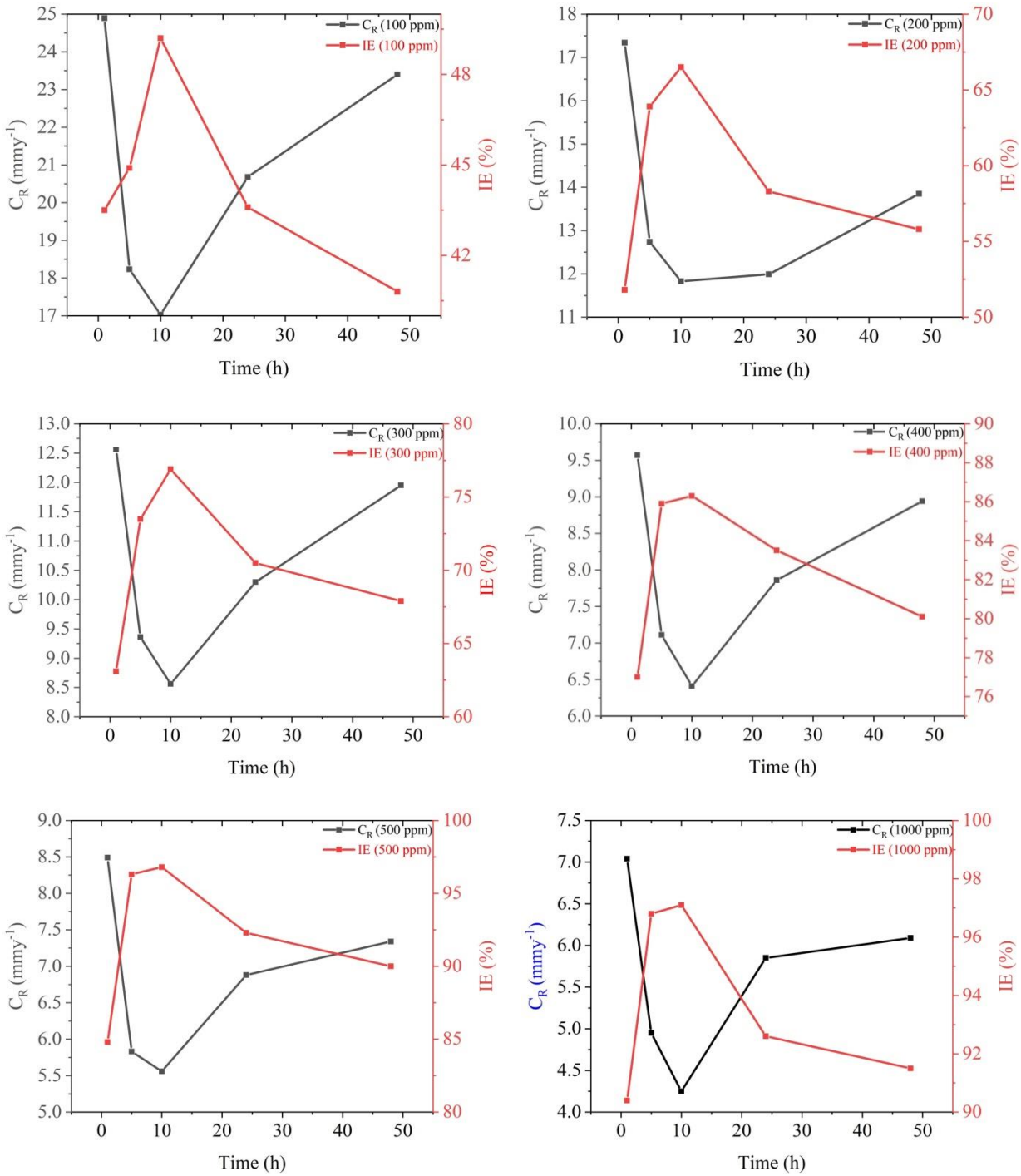

Figure 2: C_R and IE% plotted against immersion time.

The inhibitory efficiency of *P*-CBHM was also compared to other published inhibitors (Table 2), showing that *P*-CBHM has the highest inhibitory activity of the inhibitors listed [38-43], and performance comparable to that stated in [44, 45]. The corrosion rate decreased and the corrosion inhibition performance increased as the concentration of *P*-CBHM increased, possibly due to the increased adsorption coverage on the steel surface.

3.2. Effect of temperature

The corrosion inhibition was investigated at different temperatures (303 to 333 K) as shown in Figure 3. The increase in temperature increased the C_R in the presence of *P*-CBHM, with the maximum inhibitory efficacy of 96.5 % observed for 500 ppm *P*-CBHM at 303 K and 5 h immersion. The IE % reduces with increasing temperature as the generated layer (*P*-CBHM molecules) on the sample surface at 333 K has low protective ability [46, 47].

Table 2: A comparison of the corrosive inhibitory performance of *P*-CBHM to other previously published organic inhibitors.

Corrosion inhibitor	Metal	Acid	IE%	Ref.
para-chlorobenzoylhydrazinylmethane	Mild steel	HCl	96.5	-
N'-(2-(2-oxomethylpyrrol-1-yl)ethyl)piperidine	Mild steel	HCl	91.9	46
2-Amino-4-phenyl-N-benzylidene-5-(1,2,4-triazol-1-yl)thiazole	Mild steel	HCl	98.1	47
2-amino-4-phenylthiazole	Mild steel	HCl	94.7	47
1-Amino-2-mercapto-5-(4-(pyrrol-1-yl)phenyl)-1,3,4-triazole	Mild steel	HCl	96.3	48
N'-(2-hydroxybenzylidene)-2-(quinolin-8-yloxy)acetohydrazide	Mild steel	HCl	93.4	49
3-(4-ethyl-5-mercapto-1, 2, 4-triazol-3-yl)-1- phenylpropanone	Mild steel	HCl	97	50
4-ethyl-1-(4-oxo-4-phenylbutanoyl)thiosemicarbazide	Mild steel	H_2SO_4	88.7	51
4-benzyl-1-(4-oxo-4-phenylbutanoyl)thiosemicarbazide	Mild steel	HCl	92.5	52
4-chloro-2-((pyridin-2-ylimino)methyl)phenol	Low carbon steel	HCl	92.8	53
2-N-phenylamino-5-(3-phenyl-3-oxo-1-propyl)-1,3,4-oxadiazole	Mild steel	HCl	95.1	54
4-ethyl-1-(4-oxo-4-phenylbutanoyl)thiosemicarbazide	Mild steel	H_2SO_4	88.7	55
4-ethyl-1-(4-oxo-4-phenylbutanoyl)thiosemicarbazide	Mild steel	HCl	96.1	55
4-pyrrol-1-yl-n-(2,5-dimethyl-pyrrol-1-yl)benzoylamine	Mild steel	HCl	95.8	56

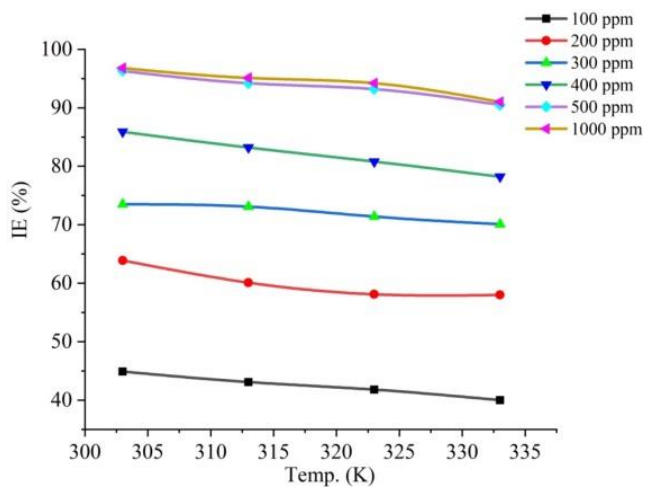

Figure 3: Inhibition efficiency plotted against temperature.

3.3. Adsorption isotherms

The surface coverage (θ) of the *P*-CBHM molecules on the steel surface was determined based on weight loss measurements and fitted by the Langmuir isotherm as follows (Eq. 10) [48, 49]:

$$\frac{C}{\theta} = \frac{1}{K_{ads}} + C \quad (10)$$

Where C represents the *P*-CBHM concentration and K_{ads} refers to the equilibrium constant.

Figure 4 shows the linear relationship between $\frac{C}{\theta}$ and C with a regression coefficient (R2) of 0.9974, which signifies that the adsorption of *P*-CBHM on the tested surface follows the Langmuir isotherm. Moreover, the K_{ads} was determined based on the intercept to calculate the adsorption free energy (ΔG^{o}_{ads}) based on Eq. 11 [50-53]:

$$\Delta G^{o}_{ads} = -2.303\ RT \log 55.5\ K_{ads} \quad (11)$$

Where R represents the constant of universal gas and T refers to the temperature in Kelvin.

The ΔG^{o}_{ads} is -33.78 kJ.mol^{-1}, with the negative charge referring to the spontaneous process and the ΔG^{o}_{ads} from -40 to -20 kJ.mol^{-1}indicates that the adsorption of *P*-CBHM on the mild steel surface occurs by physisorption and chemisorption. The physisorption mechanism suggests that the interaction accrues between the surface of mild steel and aromatic ring and/pi-bond, whereas the chemisorption mechanism occurs between unpaired elections of O and N heteroatoms in the *P*-CBHM molecule with empty iron d-orbitals on the sample surface adsorbing through interactions of the active sites and iron d-orbitals [54-56].

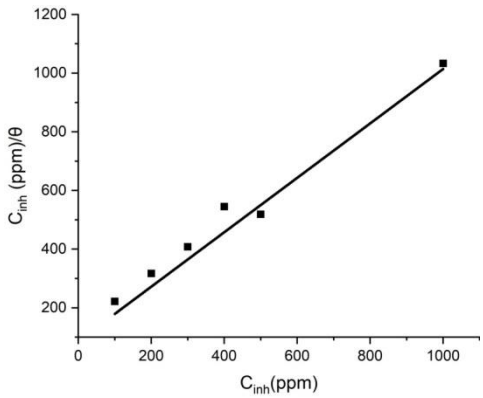

Figure 4: The plot of inhibition concentration versus $\frac{C}{\theta}$..

3.4. Quantum chemical computations

The eigenvalues of the highest occupied (HOMO) and lowest unoccupied (LUMO) molecular orbitals, the HOMO–LUMO gap, electronegativity, chemical hardness, dipole moment, Fukui indices, and other parameters are the most popular molecular-electronic properties in the inhibition-efficiency correlation approach. The molecular-electronic properties of the inhibition-efficiency correlation method are based on two assumptions. The first is that these chemical characteristics are crucial reactivity markers that can be used to forecast the direction of inhibitor adsorption bonding. The higher the eigenvalue of HOMO, the greater the molecular electron donation to the metal substrate, and the lower the eigenvalue of LUMO, the greater the electron back-donation from surface states to the molecule; however, high and low imply a small HOMO–LUMO gap because ELUMO is larger than E_{HOMO} [30-32]. The density functional theory with B3LYP at the basis set 6–31G* was used for the quantum chemical computations (Table 3). Frontier MO energies, such as E_{HOMO} and E_{LUMO}, are crucial in predicting reactive chemical species and the ability to donate an electron is associated with E_{HOMO} (Figure 5), thus an increase in E_{HOMO} suggests a stronger proclivity to donate electrons to the proper acceptor with an unoccupied orbital. E_{HOMO} facilitates the absorption of protective particles on the metal surface, with the inhibitor efficiency increased by the increased formation of an adsorbent film.

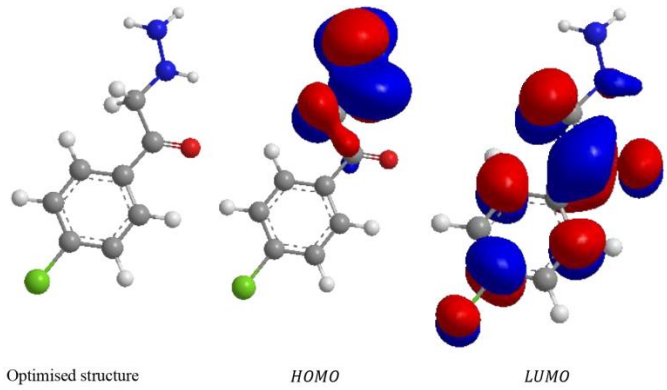

Figure 5: Optimised geometrical structure, HOMO an LUMO d of *P-CBHM.*

Table 3: Computational chemical parameters of the test inhibitor.

Computational chemical parameters	*P-CBHM*
$E_{HOMO}\ (eV)$	-6.569
$E_{\mathrm{LUMO}}\ (eV)$	−3.933
$\Delta E = E_{HOMO} - E_{LUMO}\ (eV)$	2.636
Dipole moment (μ) (D)	0.7
Global hardness (η)	1.316
Global softness (σ)	0.759
Electronegativity (χ)	5.252
Fraction of electron transfer (ΔN)	0.17

The observed quantum chemistry data validates both the physisorption and chemisorption methods, as evidenced by the negative E_{HOMO} and other thermodynamic features. Since the energy gap is related to the softness and/or hardness of the inhibitor molecules, previous investigations have shown that a high ΔE implies that the inhibitor molecules have poor reactivity [31-33], so a soft molecule with a smaller energy gap is less reactive than a hard molecule.

The ΔE dipole moment (μ) indicates a significant IE % of the inhibitor to prevent the corrosion of mild steel in 1 M HCl. Many researchers believe that heteroatoms with a strong negative charge can be adsorbed on the mild steel surface via the donors-acceptors reaction mechanism [30-34]. Moreover, a low degree of electronegativity, a large molecular weight, and a low ΔE promote efficient adsorption of the inhibitor molecules on the MS surface, thereby reducing corrosion. The ΔN value in Table 3 shows that the examined inhibitor molecules transport more electrons to the d-orbitals of iron atoms on the mild steel surface, thus are more efficient [30-34].

3.5. Postulated inhibitive mechanism

There are various mechanisms by which organic inhibitors can prevent the corrosion of metal in an acidic environment. *P*-CBHM molecules can adsorb via the lone pairs in the heterocyclic rings and other functional groups to the unoccupied d-orbitals of iron atoms on the mild steel surface, with the protection efficiency depending on the chemical adsorption and physical adsorption (Figure 6). The N and O atoms in the inhibitor molecule operate as adsorption sites, with the unpaired electrons used to establish coordination bonds and chemisorb onto the mild steel surface. The protonation of nitrogen atoms is simple and can be accomplished through physisorption with chloride ions. The presence of unpaired electrons and the inductive impact of methylene groups are responsible for the prevention of corrosion. Chemisorption techniques can be utilized to characterise *P*-CBHM molecule adsorption on mild steel substrates and the activity of *P*-CBHM on the sample surface can be described based on the following equations (Eqs. 12-14):

$$Fe + P\text{-}CBHM \leftrightarrow Fe(P\text{-}CBHM)_{ads} \quad (12)$$

$$Fe(P-CBHM)_{ads} \leftrightarrow Fe^{++} + P-CBHM + ne^{-} \quad (13)$$

$$(P-CBHM)_{aq} + H_2O_{ads} \leftrightarrow (P-CBHM)_{ads} + H_2O_{aq} \quad (14)$$

Donor/acceptor interactions between N and O unpaired electrons of *P*-CBHM with the empty iron d-orbitals on the sample surface allow the chemical adsorption of *P*-CBHM molecules on the sample surface. The ΔG^{o}_{ads} for the tested inhibitor is -33.78 kJ.mol^{-1}, demonstrating that the *P*-CBHM adsorption mechanism on the mild steel surface is a combination of physisorption and chemisorption [30].

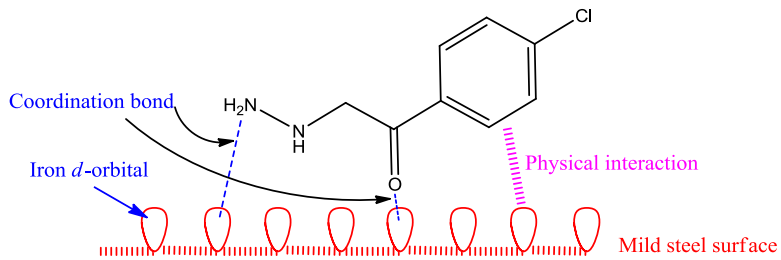

Figure 6: The postulated mechanism of P-CBHM prevention of corrosion on the mild steel surface in 1 M HCl.

3.6. Antibatcterial effects

Antibacterial resistance of novel disease-causing microorganisms is increasing [57], with pathogens in the maritime environment causing infectious diseases in humans and aquaculture organisms, posing serious health risks and financial losses. Furthermore, the increased and indiscriminate use of antibiotics has led to the development of resistance to antibiotics, as well as hypersensitivity and a loss of beneficial microorganisms in the human gut. Consequently, several bioactive and pharmacologically significant molecules have been developed as commercially available medications and there is an increased demand for new, environmentally friendly antipathogenic, antifoulant, and anticorrosion materials. The antimicrobial activity of *P*-CBHM was assessed using the disc diffusion assay (Figure 7), showing that *P*-CBHM was more effective against the gram-positive *S. aureus*, with the inhibitory activity increasing with concentration [57] and linked to nitrogen atoms. The *P*-CBHM demonstrated strong inhibitory activity against all tested microorganisms but was less effective than commonly used chloramphenicol.

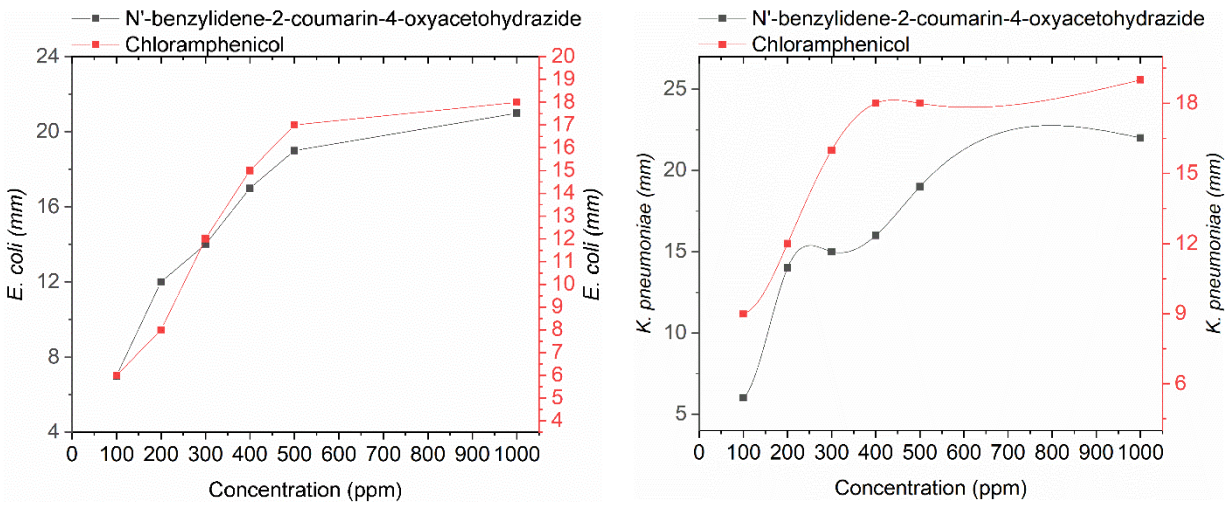

Figure 7: Antimicrobial efficiency of different concentrations of *P*-CBHM compared to chloramphenicol.

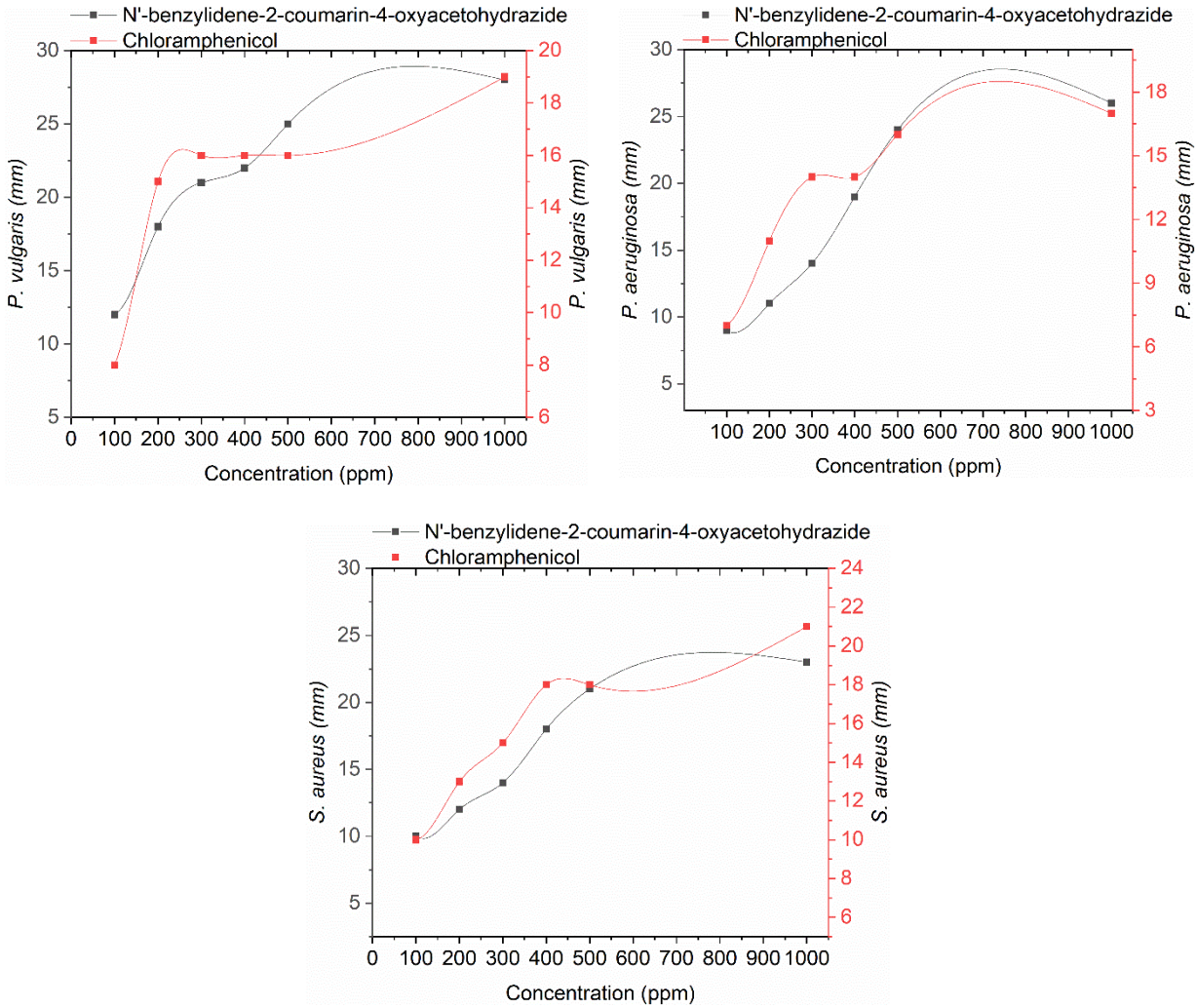

Figure 7: Continiue

4. Conclusion

The new hydrazine derivative *P*-CBHM significantly inhibited the corrosion of mild steel in 1 M HCl solution due to the numerous highly efficient electronic adsorption sites including oxygen, nitrogen, chloro, and carbonyl that interacted with the iron active sites via physisorption and chemisorption mechanisms. P-CBHM also demonstrated antibacterial activity against gram-negative and gram-positive bacteria. In the conclusion, some perspective related to future research work, where the tested corrosion inhibitor will be studied using electrochemical techniques, in addtion to use of other types of alloys.

5. References

1. A. Al-Amiery, L. Shaker, A. Kadhum, M. Takriff, Corrosion inhibition of mild steel in strong acid environment by 4-((5,5-dimethyl-3-oxocyclohex-1-en-1-yl)amino)benzenesulfonamide, *Tribol. Ind.*, 42(2020), 89-101.
2. K. Aly, A. Mahdy, M. Hegazy, N. Al-Muaikel, S. Kuo, M. Gamal Mohamed, Corrosion resistance of mild steel coated with phthalimide-functionalized polybenzoxazines, *Coatings*, 10(2020), 1114.
3. A. Al-Amiery, T. Salman, K. Alazawi, L. Shaker, A. Kadhum, M. Takriff, Quantum chemical elucidation on corrosion inhibition efficiency of Schiff base: DFT investigations supported by weight loss and SEM

techniques, *Int. J. Low Carbon Technol.*, 15(2020), 202-209.
4. A. Al-Amiery, L. Shaker, A. Kadhum, M. Takriff, Synthesis, characterization and gravimetric studies of novel triazole-based compound, *Int. J. Low Carbon Technol.*, 15(2020), 164-170.
5. K. Aly, M. Mohamed, O. Younis, M. Mahross, M. Abdel-Hakim, M., Sayed, Salicylaldehyde azine-functionalized polybenzoxazine: Synthesis, characterization, and its nanocomposites as coatings for inhibiting the mild steel corrosion, *Prog. Org. Coat.*, 138(2020), 105385.
6. K. Aly, O. Younis, M. Mahross, E. Orabi, M. Abdel-Hakim, O. Tsutsumi, M. Sayed, Conducting copolymers nanocomposite coatings with aggregation-controlled luminescence and efficient corrosion inhibition properties, *Prog. Org. Coat.*, 135(2019), 525-535.
7. A. Al-Amiery, A. Kadhum, A. Kadihum, A., Mohamad, C. How, S. Junaedi, Inhibition of mild steel corrosion in sulfuric acid solution by new schiff base, *Mater.*, 7(2014), 787-804.
8. A. Al-Amiery, L. Shaker, Corrosion inhibition of mild steel using novel pyridine derivative in 1 M hydrochloric acid, *Koroze Ochr. Mater*., 64(2020), 59-64.
9. A. Al-Amiery, Anti-corrosion performance of 2-isonicotinoyl-n-phenylhydrazinecarbothioamide for mild steel hydrochloric acid solution: Insights from experimental measurements and quantum chemical calculations, *Surf. Rev. Lett.*, 28(2021), 1-8.
10. M. Mohamed, S. Kuo, A. Mahdy, I. Ghayd, K. Aly, Bisbenzylidene cyclopentanone and cyclohexanone-functionalized polybenzoxazine nanocomposites: Synthesis, characterization, and use for corrosion protection on mild steel, *Mater. Today Commun.*, 25(2021), 101418.
11. M. Mohamed, A. Mahdy, R. Obaid, M. Hegazy, S. Kuo, K. Aly, Synthesis and characterization of polybenzoxazine/clay hybrid nanocomposites for UV light shielding and anti-corrosion coatings on mild steel, *J. Polym. Res.*, 28(2021), 297.
12. S. Al-Baghdadi, T. Gaaz, A. Al-Adili, A., Al-Amiery, M. Takriff, Experimental studies on corrosion inhibition performance of acetylthiophene thiosemicarbazone for mild steel in HCl complemented with DFT investigation, *Int. J. Low Carbon Technol.*, 16(2021), 181-188.
13. S. Al-Baghdadi, F. Hashim, A. Salam, T. Abed, T. Gaaz, A. Al-Amiery, A. Kadhum, K. Reda, W. Ahmed, Synthesis and corrosion inhibition application of NATN on mild steel surface in acidic media complemented with DFT studies, *Results Phys.*, 8(2018) 1178-1184.
14. S. Al-Baghdadi, A. Al-Amiery, A. Kadhum, M. Takriff, Computational calculations, gravimetrical, and surface morphological investigations of corrosion inhibition effect of triazole derivative on Mild Steel in HCl, *J. Comput. Theor. Nanosci.*, 17(2020), 4797-4804.
15. S. Al-Baghdadi, A. Kadhim, G. Sulaiman, A. Al-Amiery, A. Kadhum, M. Takriff, Anticorrosion and antibacterial effects of new Schiff base derived from hydrazine, *J. Phys. Conf. Ser.*, 1795(2021), 012021.1
16. S. Al-Taweel, T. Gaaz, L. Shaker, A. Al-Amiery, Protection of mild steel in h2so4 solution with 3-((3-(2-hydroxyphenyl)-5-thioxo-1,2,4-triazol-4-yl)imino)indolin-2-one, *Int. J. Corros. Scale Inhib.*, 9(2020), 1014-1024.
17. A. Alamiery, E. Mahmoudi, T. Allami, Corrosion inhibition of low-carbon steel in hydrochloric acid environment using a Schiff base derived from pyrrole : gravimetric and computational studies, *Int. J. Corros. Scale Inhib.*, 10(2021), 749-765.
18. A. Alamiery, L. Shaker, T. Allami, A. Kadhum, S. Takriff, A study of acidic corrosion behavior of Furan-Derived schiff base for mild steel in hydrochloric acid environment: Experimental, and surface investigation, *Mater. Today*, 44(2021), 2337-2341.
19. M. Mohamed, A. Mahdy, R. Obaid, Synthesis and characterization of polybenzoxazine/clay hybrid nanocomposites for UV light shielding and anti-corrosion coatings on mild steel, *J. Polym. Res.*, 28(2021), 297.
20. ASTM International, Standard Practice for Preparing, Cleaning, and Evaluating Corrosion Test, (2011), 1-9
21. A. Eltmimi, A. Alamiery, T. Allami, M. Yusop, Inhibitive effects of a novel efficient Schiff base on mild steel in hydrochloric acid environment, *Int. J. Corros. Scale Inhib.*, 4(2021), 634-648.
22. H. Habeeb, H. Luaibi, T. Abdullah, R. Dakhil, A. Kadhum, A. Al-Amiery, Case study on thermal impact of novel corrosion inhibitor on mild steel, *Case Stud. Therm. Eng.*, 12(2018), 64-68.
23. H. Habeeb, H. Luaibi, R. Dakhil, A. Kadhum, A. Al-Amiery, T. Gaaz, Development of new corrosion inhibitor tested on mild steel supported by electrochemical study, *Results Phys.*, 8 (2018), 1260-1267.
24. M. Hanoon, A. Resen, L. Shaker, A. Kadhum, A. Al-Amiery, Corrosion investigation of mild steel in aqueous hydrochloric acid environment using n-(Naphthalen-1yl)-1-(4-pyridinyl)methanimine complemented with antibacterial studies, *Biointerface Res. Appl. Chem.*, 11 (2021), 9735-9743.
25. M. Hanoon, D. Zinad, A. Resen, A. Al-Amiery, Gravimetrical and surface morphology studies of corrosion inhibition effects of a 4-aminoantipyrine derivative on mild steel in a corrosive solution, *Int. J. Corros. Scale Inhib.*, 9 (2020), 953-966.
26. D. Jamil, A. Al-Okbi, S. Al-Baghdadi, A. Al-Amiery, A. Kadhim, T. Gaaz, A. Kadhum, A. Mohamad, Experimental and theoretical studies of Schiff bases as corrosion inhibitors, *Chem. Cent. J.*, 12(2018), 1-9.
27. Q. Jawad, A. Hameed, M. Abood, A. Al-Amiery, L. Shaker, A. Kadhum, M. Takriff, Synthesis and comparative study of novel triazole derived as

corrosion inhibitor of mild steel in hcl medium complemented with calculations, *Int. J. Corros. Scale Inhib.*, 9(2020), 688-705.
28. S. Junaedi, A. Al-Amiery, A. Kadihum, A. Kadhum, A. Mohamad, Inhibition effects of a synthesized novel 4-aminoantipyrine derivative on the corrosion of mild steel in hydrochloric acid solution together with quantum chemical studies, *Int. J. Mol. Sci.*, 14(2013), 11915-11928.
29. S. Junaedi, A. Kadhum, A. Al-Amiery, A. Mohamad, M. Takriff, Synthesis and characterization of novel corrosion inhibitor derived from oleic acid: 2-Amino 5-Oleyl-1,3,4-Thiadiazol (AOT), *Int. J. Electrochem. Sci.*, 7(2012), 3543-3554.
30. S. Junaedi, A. Al-Amiery, A. Kadihum, A. Kadhum, A. Mohamad, Inhibition effects of a synthesized novel 4-aminoantipyrine derivative on the corrosion of mild steel in hydrochloric acid solution together with quantum chemical studies, *Int. J. Mol. Sci.*, 14(2013), 11915-11928.
31. H. Obayes, A. Al-Amiery, G. Alwan, T. Abdullah, A. Kadhum, A. Mohamad, Sulphonamides as corrosion inhibitor: Experimental and DFT studies, *J. Mol. Struct.*, 1138(2017), 1-9.
32. E. Sheet, J. Yamin, H. Al-Salihi, A. Salam, K. Reda, W. Ahmed, M. Mahdi, A. Al-Amiery, N-(3-nitrobenzylidene)-2-aminobenzothiazole as new locally available corrosion inhibitor for iraqi oil industry, *J. Balk. Tribol. Assoc.*, 26(2020), 194-203.
33. J. Yamin, E. Sheet, A. Al-Amiery, Statistical analysis and optimization of the corrosion inhibition efficiency of a locally made corrosion inhibitor under different operating variables using RSM, *Int. J. Corros. Scale Inhib.*, 9(2020), 502-518.
34. D. Zinad, M. Hanoon, R. Salim, S. Ibrahim, A. Al-Amiery, M. Takriff, A. Kadhum, A new synthesized coumarin-derived schiff base as a corrosion inhibitor of mild steel surface in hcl medium: Gravimetric and studies, *Int. J. Corros. Scale Inhib.*, 9(2020), 228-243.
35. A. Hilchie, K. Wuerth, R.Hancock, Immune modulation by multifaceted cationic host defense (antimicrobial)peptides. *Nat. Chem. Biol*. 9(2013), 761–768.
36. Kadhim, A. Al-Amiery, R. Alazawi, M. Al-Ghezi, R. Abass, Corrosion inhibitors. A review. Int. J. Corros. Scale Inhib., 10(2021), 54–67.
37. Kadhim, A. Al-Okbi, D. Jamil, A. Qussay, A. Al-Amiery, T. Gaaz, A. Kadhum, A. Mohamad, M. Nassir, Experimental and theoretical studies of benzoxazines corrosion inhibitors. Results Phys., 7(2017), 4013–4019.
38. Kadhim, G. Sulaiman, A. Abdel Moneim, R. Yusop, A. Al-Amiery, Synthesis and characterization of triazol derivative as new corrosion inhibitor for mild steel in 1M HCl solution complemented with antibacterial studies. J. Phys. Conf. Ser., 1795(2021), 012011.
39. D. Zinad, Q. Jawad, M. Hussain, M. Mahal, L. Mohamed, A. Al-Amiery, Adsorption, temperature and corrosion inhibition studies of a coumarin derivatives corrosion inhibitor for mild steel in acidic medium: Gravimetric and theoretical investigations. Int. J. Corros. Scale Inhib., 9(2020), 134–151.
40. A. Resen, M. Hanoon, W. Alani, A. Kadhim, A., Mohammed, T. Gaaz, A. Kadhum, A. Al-Amiery, M. Takriff, Exploration of 8-piperazine-1-ylmethylumbelliferone for application as a corrosion inhibitor for mild steel in hydrochloric acid solution, *Int. J. Corros. Scale Inhib.*, 10(2021), 368-387.
41. Salim, Q. Jawad, K. Ridah, L. Shaker, A. Al-Amiery, A. Kadhum, M. Takriff, Corrosion inhibition of thiadiazole derivative for mild steel in hydrochloric acid solution, *Int. J. Corros. Scale Inhib.*, 9(2020), 550-561.
42. Salman, Q. Jawad, K. Ridah, L. Shaker, A. Al-Amiery, Selected bis-thiadiazole: synthesis and corrosion inhibition studies on mild steel in HCl environment, *Surf. Rev. Lett.*, 27(2020), 1-5.
43. T. Salman, Q. Jawad, M. Hussain, A. Al-Amiery, L. Mohamed, A. Kadhum, M. Takriff, Novel ecofriendly corrosion inhibition of mild steel in strong acid environment: Adsorption studies and thermal effects, *Int. J. Corros. Scale Inhib.*, 8(2019), 1123-1137.
44. T. Salman, Q. Jawad, M. Hussain, A. Al-Amiery, L. Shaker, A. Kadhum, M. Takriff, New environmental friendly corrosion inhibitor of mild steel in hydrochloric acid solution: Adsorption and thermal studies, *Cogent Eng.*, 7(2020), 1826077.
45. L. Shaker, A. Al-Adili, A. Al-Amiery, M. Takriff, The inhibition of mild steel corrosion in 0.5 M H_2SO_4 solution by N-phenethylhydrazinecarbothioamide (N-PHC), *J. Phys. Conf. Ser.*, 1795(2021), 012009.
46. A. Alamiery, Study of corrosion behavior of N'-(2-(2-oxomethylpyrrol-1-yl) ethyl) piperidine for mild steel in the acid environment, *Biointerface Res. Appl. Chem.*, 12(2022), 3638-3646
47. Alamiery, A. Mohamad, A. Kadhum, M. Takriff, Comparative data on corrosion protection of mild steel in HCl using two new thiazoles, *Data Brief*, 40(2022), 107838
48. A.M. Mustafa, F.F. Sayyid, N. Betti, L.M. shaker, M.M. Hanoon, A.A. Alamiery, A.A.H. Kadhum, M.S. Takriff, Inhibition of mild steel corrosion in hydrochloric acid environment by 1-amino-2-mercapto-5-(4-(pyrrol-1-yl)phenyl)-1,3,4-triazole, *S. Afr. J. Chem. Eng*., 39(2022), 42-51.
49. A. Alamiery, Investigations on corrosion inhibitory effect of newly quinoline derivative on mild steel in HCl solution complemented with antibacterial studies, *Biointerface Res. Appl. Chem.*, 12(2022), 1561-1568
50. A. Alkadir Aziz, A. A. Annon, M. Abdulkareem, M Hanoon, M. Alkaabi, L. Shaker, A. Alamiery, W.N.R. Wan Isahak, M. Takriff, Insights into corrosion inhibition behavior of a 5-mercapto-1,2,4-triazole derivative for mild steel in hydrochloric acid solution: experimental and DFT studies, *Lubricants*, 9(2021), 1-14.

51. A. Alamiery, Short report of mild steel corrosion in 0.5 M H_2SO_4 by 4-ethyl-1-(4-oxo-4-phenylbutanoyl) thiosemicarbazide, *J. Tribolog*, 30(2021), 90-99.
52. Alamiery, W.N.R.W. Isahak, M. Takriff, Inhibition of mild steel corrosion by 4-benzyl-1-(4-oxo-4-phenylbutanoyl)thiosemicarbazide: Gravimetrical, adsorption and theoretical studies, *Lubricants*, 9(2021), 1-10.
53. M.A. Dawood, Z.M.K. Alasady, M.S. Abdulazeez, D.S. Ahmed, G.M. Sulaiman, A.A.H. Kadhum, L.M. Shaker6 and A.A. Alamiery, The corrosion inhibition effect of a pyridine derivative for low carbon steel in 1 M HCl medium: Complemented with antibacterial studies, *Int. J. Corros. Scale Inhib.*, 10(2021), 1766-1782.
54. A. Alamiery, Corrosion inhibition effect of 2-N-phenylamino-5-(3-phenyl-3-oxo-1-propyl)-1,3,4-oxadiazole on mild steel in 1 M hydrochloric acid medium: Insight from gravimetric and DFT investigations, *Mater. Sci. Technol.*, 4(2021), 398-406.
55. Alamiery, A.A. Anticorrosion effect of thiosemicarbazide derivative on mild steel in 1 M hydrochloric acid and 0.5 M sulfuric Acid: Gravimetrical and theoretical studies, *Mater. Sci. Technol.*, 4(2021), 263-273.
56. Alamiery, W.N.R.W. Isahak, H., Aljibori, H. Al-Asadi, A. Kadhum, Effect of the structure, immersion time and temperature on the corrosion inhibition of 4-pyrrol-1-yl-n-(2,5-dimethyl-pyrrol-1-yl)benzoylamine in 1.0 m HCl solution, *Int. J. Corros. Scale Inhib.*, 10 (2021), 700-713.
57. Al-Amiery, A. Kadhum, A. Mohamad, Antifungal activities of new coumarins, *Molecules*, 17(2012), 5713-5723.

How to cite this article:
S. S. Hussein, I. D. D. Al-Hasani, A. M. Abed, M. M Hanoon, L. M. Shaker, A. A. Alamiery, A. A. H. Kadhum, Wan Nor Roslam Wan Isahak, Antibacterial Corrosion Inhibitor for the Protection of Mild Steel in 1 M HCl Solution. Prog. Color Colorants Coat., 16 (2023), 59-70.